

See discussions, stats, and author profiles for this publication at: <https://www.researchgate.net/publication/230557051>

Surface Chemistry and Spectroscopy of Human Insulin Langmuir Monolayer

ARTICLE in THE JOURNAL OF PHYSICAL CHEMISTRY B · AUGUST 2012

Impact Factor: 3.3 · DOI: 10.1021/jp3046643

CITATIONS

12

READS

44

9 AUTHORS, INCLUDING:



Garima Thakur

University of Alberta

21 PUBLICATIONS 194 CITATIONS

SEE PROFILE



Jhony Orbulescu

MP Biomedicals

52 PUBLICATIONS 979 CITATIONS

SEE PROFILE



Roger M Leblanc

University of Miami

165 PUBLICATIONS 3,732 CITATIONS

SEE PROFILE

Surface Chemistry and Spectroscopy of Human Insulin Langmuir Monolayer

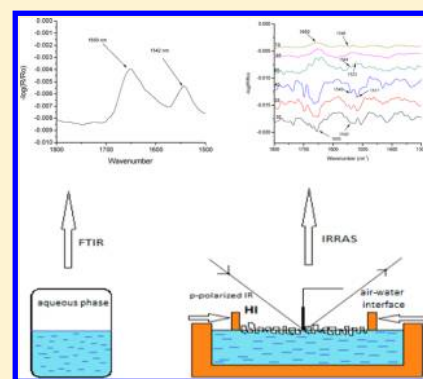
Sheba Johnson,[†] Wei Liu,[†] Garima Thakur,[†] Anup Dadlani,[†] Ravi Patel,[†] Jhony Orbulescu,^{†,‡} Jeffrey D. Whyte,[‡] Miodrag Micic,^{‡,§} and Roger M. Leblanc^{*,†}

[†]Department of Chemistry, University of Miami, 1301 Memorial Drive, Department of Chemistry, Coral Gables, Florida, 33146, United States

[‡]MP Biomedicals LLC, 3 Hutton Center, Santa Ana, California 92707, United States

[§]Department of Mechanical and Aerospace Engineering, University of California, Irvine, 4200 Engineering Gateway Building, Irvine, California 92697-3975, United States

ABSTRACT: The human insulin (HI) protein was examined to elucidate its structure at the air–water interface. Optimal experimental conditions were determined to prepare a homogeneous and stable human insulin (HI) Langmuir monolayer. HI insulin Langmuir monolayer can be used to study interactions of HI with a membrane as Langmuir monolayers are used as an in vitro model of biological membranes. Surface pressure and surface potential–area isotherms were used to characterize the HI Langmuir monolayer. The compression–decompression cycles and stability measurements showed a homogeneous and stable monolayer at the air–water interface. However, higher surface pressures resulted in a higher decrease in area and less stability. In situ UV–vis and fluorescence spectroscopy were used to verify the homogeneity of the HI monolayer and to identify the chromophore residues in the HI. Domain formation was examined through epifluorescence and Brewster angle microscopies. The conformation of HI was examined by circular dichroism (CD) and Fourier transform infrared spectroscopy (FTIR) in the aqueous phase and at the air–water interface by infrared reflection absorption spectroscopy (IRRAS). HI was found to exist as a monomer in 2-D.



1. INTRODUCTION

Human insulin (HI) is a peptide hormone which is produced in islets of Langerhans, and its main function in the human body is to control blood glucose level. Since the discovery of insulin, diabetes has become treatable. HI is composed of two polypeptide chains, an A chain with 21 residues and a B chain with 30 residues, linked together by two disulfide bonds.¹

Besides the monomeric structure of HI, it is also found to exist as dimers, hexamers, and amyloids. As a monomer, the majority of the structure of HI is composed of an α -helical structure and it dimerizes through the formation of β -sheet.² HI is often found having a dimer structure which is due to hydrogen bonding between the C terminus of B chains. HI dimers come together to form hexamers in the presence of zinc ions.³ Monomers and dimers readily diffuse into blood, whereas hexamers diffuse poorly. Hence, absorption of HI preparations containing a high proportion of hexamers is delayed and somewhat slow.⁴ HI amyloid is characterized by β sheet.⁵ Tissue deposition of normally soluble proteins as insoluble amyloid fibrils is associated with serious diseases including the systemic amyloidoses, maturity onset diabetes, and Alzheimer's disease.⁶ In vitro, HI is readily converted to an inactive fibrillar form by incubation at high HI concentrations, low pH, and high temperatures.⁵

Interactions of proteins like HI with human cellular membrane can be studied by using Langmuir monolayer

methodology.⁶ Langmuir monolayers are used as an in vitro model of biological membranes.⁷ This technique allows us to study intermolecular interactions between molecules spread at the interface which form the monolayer. In this method, HI dissolved in acidic solution is first spread onto a water surface to form the Langmuir or floating monolayer. Monolayer formation is usually monitored with the surface pressure (π)–area (A) isotherm.^{8–10} Surface pressures ranging between 30 and 35 mN/m are commonly found in the natural biomembrane and can be simulated on the Langmuir monolayer to mimic human cell membrane.⁷ One of the earliest studies employing this technique was published in 1954, and it reported the change in insulin surface pressure with change in pH.¹¹ A series of studies on insulin Langmuir monolayer reported the effect of temperature, monolayer composition, and nature of cations in the subphase.^{3,12–17} Insulin Langmuir–Blodgett (LB) films on mica slides have also been studied by atomic force microscopy (AFM).¹⁸

The present study brings new data on the optical properties of the HI Langmuir monolayer. UV–vis at the air–water interface correlates with the surface pressure–area isotherm curve. Domain formation in 2-D was not observed on the basis

Received: May 14, 2012

Revised: July 20, 2012

Published: July 26, 2012

of the Brewster angle and epifluorescence microscopies of HI and FITC-labeled HI Langmuir monolayer, respectively. One has observed through IRRAS measurements that the protein conserves an α -helix conformation in 2-D, knowing that the IRRAS approach permits detection of the amide I and amide II bands, which correlates with the α -helix and β -sheet in the protein sample.^{19,20}

2. EXPERIMENTAL SECTION

2.1. Materials. Pure recombinant human insulin, methanol, chloroform, and hydrochloric acid were obtained from MP Biomedicals, LLC (Solon, OH). The recombinant human insulin (Catalog# 199744, 99.3% assay) has been produced in *E. coli* expression system and purified using affinity purification. All chemicals were reagent grade and were used without any further purification. The water utilized for subphase preparation was obtained from a Modulab 2020 water purification system (Continental Water System Corp., San Antonio, TX). The purified water has a surface tension of 72.6 mN·m⁻¹ at 20.0 ± 0.5 °C, resistivity of 18 MΩ·cm, and pH 5.6.

2.2. Methods. Procedure for FITC-Human Insulin Conjugation. The topography of the HI Langmuir monolayer was examined through epifluorescence of the FITC-HI. Since insulin is nonfluorescent, one must attach a fluorophore to make use of the epifluorescence microscopy. The commonly used probe for proteins is fluorescein isothiocyanate (FITC).

The FITC conjugated HI was prepared the following way. FITC (1 mg/mL) and HI (0.3 mg/mL) solutions were made separately in PBS solution. FITC solution and any solutions containing FITC was covered with aluminum foil to prevent photodegradation of the fluorescent probe. FITC solution was added to insulin solution dropwise and stirred for an hour. Both solutions were mixed with each other in molar ratios between FITC:insulin ranging from 0.5:1 to 4:1. After stirring, the solution was run through a G-25 Sephadex column (globular protein range: 1 × 10³ to 5 × 10³ Da) to separate according to the weight in the following order: FITC-HI, HI, and FITC. When the mass of one of the components flowing thorough the Sephadex column is higher than the range, those components will flow out first. The maximum range of G-25 Sephadex is 5000 Da; however, HI's molar mass is 5870 g mol⁻¹. Two out of the three components were higher than 5000 Da, namely, the HI-FITC and HI. Thus, the heaviest component, which is HI-FITC, will flow out of the column first, followed by HI. The lightest component is FITC and FITC fragments, which remain at the very top of the column as seen by the bright green luminescence at the top of the column. Shining UV light on the column shows three distinct regions: a fluorescent green region near the base of the column which corresponds to FITC-HI, a nonfluorescent part above it which corresponds to the HI not conjugated to FITC and a fluorescent yellow region at the top of the column corresponding to FITC not conjugated to HI. PBS buffer was used to run the column, and aliquots were collected in volumes of 1 mL.

Fluorescence spectroscopy was used to select the aliquots containing FITC-HI. FITC probe showed an emission at 517 nm when excited at 494 nm. One has noted that the intensity of the FITC emission increases when the probe is conjugated to HI. Absorption spectroscopy was used to determine the ratio of HI to FITC, which was calculated from the following equation.²¹

$$\frac{A_{495} \times \epsilon_{280, \text{HI}} \times \text{MolWt}_{\text{HI}}}{389 \times \epsilon_{495, \text{FITC}} \times (0.35 - A_{495})}$$

where MolWt_{HI} = 5870 g mol⁻¹ and $\epsilon_{280, \text{HI}}$ and $\epsilon_{495, \text{FITC}}$ are 17 335 and 90 000, respectively. A_{495} and A_{280} are the absorbances of the conjugate and HI at 494 and 280 nm, respectively. The correction factor taking into account the absorbance of FITC at 280 nm is 0.35 × A_{495} . Various conjugates (FITC α -HI) were prepared with α representing an average number of FITC molecules bound per HI. One has prepared 1–10 FITC molecules attached to HI molecule, but HI conjugates having 1 FITC molecule was mainly used in the epifluorescence microscopy experiments.

Langmuir Monolayer Preparation. The HI solution used in the Langmuir monolayer experiments had a concentration of 0.30 mg/mL and was prepared by dissolving HI powder in aqueous HCl solution (pH 2). For all experiments performed as a Langmuir monolayer, the subphase (pure water) was at a pH of 5.6. The volume of the spreading solution was 80 and 40 μ L for Kibron and KSV troughs, respectively. The HI solution was spread at the air–water interface, using a 100 μ L syringe (Hamilton Co., Reno, Nevada) by small droplet deposition uniformly over the subphase surface, followed by a 15 min waiting period for the Langmuir monolayer to reach equilibrium. The compression rate was set at 10 mm·min⁻¹. All the isotherms and in situ UV–vis, fluorescence, and IRRAS spectroscopic measurements were conducted in a clean room (class 1000) where temperature (20.0 ± 0.5 °C) and humidity (50 ± 1%) were kept constant.

Surface Chemistry and Spectroscopy Methods. A Kibron μ -trough (Kibron Inc., Helsinki, Finland) with an area of 5.9 cm × 21.1 cm was utilized for the surface pressure–area (π – A) isotherm, compression–decompression cycles, and stability studies. Surface potential–area (ΔV – A) isotherms were obtained on the Kibron trough using a Kelvin probe consisting of a capacitor-like system. The vibrating plate was set at approximately 1 mm above the surface of the Langmuir monolayer, and a gold-plated trough-base was used as a counter electrode.

Spectroscopic measurements at the air–water interface were obtained with an HP spectrophotometer model 8452 A for UV–vis and Fluorolog-3 spectrofluorimeter (Horiba Scientific, Edison, NJ) for fluorescence. The fluorescence spectra of HI Langmuir monolayer at the air–water interface were measured using a bifurcated optical fiber with an area of 0.25 cm² and was placed 1 mm above the surface of the subphase. The excitation light was transmitted through the optical fiber from the light source to the Langmuir monolayer, and the emission light from the Langmuir monolayer was sent back to the detector through the optical fiber. UV–vis absorption and fluorescence spectra of aqueous solutions were recorded on a Perkin-Elmer Lambda 900 UV/vis/NIR spectrometer (Norwalk, CT) and Fluorolog-3 spectrofluorimeter (same as the one used for the Langmuir monolayer) using a quartz cuvette of 1 cm optical path length, respectively.

Epifluorescence microscopy was employed to visualize the formation of domains in a Langmuir monolayer, if any. The microscope requires a Langmuir trough to be placed on top of the sample stage. A quartz window allows the excitation light to penetrate the subphase so that one could excite the fluorophore at the air–water interface. The experimental setup used a Kibron μ -trough (Kibron Inc., Helsinki, Finland) combined with an epifluorescence microscope (Olympus IX-FLA). The

area available for the spreading solution was $5.9 \text{ cm} \times 21.1 \text{ cm}$. The epifluorescence image was captured by a thermoelectrically cooled Optonics Magnafire CCD camera.

Brewster angle microscopy (BAM) was used to visualize the topography of the Langmuir monolayer. The measurements were performed using the IELI-2000 imaging ellipsometer with the compensator turned off and BAM2plus software. The standard laser of the IELI2000 system is a frequency doubled Nd:YAG laser (50 mW output) using the 532 nm line.

Circular dichroism (CD) spectra were obtained using a JASCO J-810 spectropolarimeter. The spectra were recorded between 195 and 250 nm at 25°C using a 2.0 mm optical path length quartz cell.

The infrared spectrum of an aqueous solution was obtained using attenuated total reflectance. With the Bio-ATR accessory, the aqueous sample was deposited on the ATR crystal surface, and the IR spectrum was readily obtained. The static mode required only 15–20 μL of aqueous solution; however, the concentration of the aqueous solution should be larger than 0.5 mg/mL to ensure a proper contact with the ATR crystal. A mercury–cadmium–telluride (MCT) detector (Kolmar Technologies) was used with a scanner velocity of 5 kHz. The background spectrum was pure water. The Bio-ATR cell II was placed in the cell compartment of a Bruker Optics Equinox55 FTIR.

Infrared reflection–absorption spectroscopy (IRRAS) measurements of the Langmuir monolayer were performed using an EQUINOX-55 Fourier transform infrared (FTIR) spectrometer (Bruker Optics, Billerica, MA) equipped with an XA-511 external reflection accessory suitable for the air–water interface experiments. The IR beam was focused at the air–water interface of the Kibron μ -trough. The reflected IR beam went to a HgCdTe (MCT) detector cooled by liquid nitrogen. The spectra were acquired with a resolution of 8 cm^{-1} by coaddition of 1200 scans for p-polarized and 800 scans for s-polarized IRRAS.

3. RESULTS AND DISCUSSION

3.1. Surface Pressure and Surface Potential–Area Isotherms. The surface pressure and surface potential–area isotherms of the HI Langmuir monolayer are shown in Figure 1. The lift-off of the surface pressure and surface potential correspond to 750 and $900 \text{ \AA}^2 \text{ molecule}^{-1}$, respectively. One would expect to observe a lift-off at a larger area for the surface

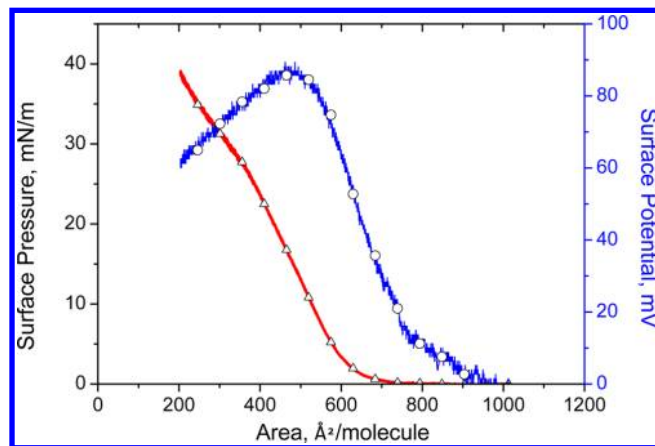


Figure 1. Surface pressure (Δ) and surface potential–area (\circ) isotherms of human insulin Langmuir monolayer at subphase pH 5.6.

potential compared with the surface pressure. This is due to the long-range interaction of the surface dipoles compared to the van der Waals interaction, which is mainly measured by the surface pressure. With regard to the limiting molecular area, that is, the extrapolation of the linear part of the surface pressure–area isotherm to zero surface pressure, a value of $620 \text{ \AA}^2 \text{ molecule}^{-1}$ is obtained. This area corresponds to the most compact state of the HI protein at the air–water interface, a value in line with previous published studies on bovine insulin Langmuir monolayer.^{3,17}

Decreasing the molecular area from 750 , one observes a gaseous to liquid expanded phase transition in the surface pressure–area isotherm. Further decrease from 585 to 350 shows the liquid condensed phase of the Langmuir monolayer. One reaches the collapse surface pressure 25.2 mN m^{-1} . The surface pressure measurement until collapse shows a linear increase in the π – A isotherm. The next section on the stability measurements will show that the HI Langmuir monolayer is stable in 2-D.

3.2. Compression–Decompression Cycles and Stability Isotherms of Human Insulin Langmuir Monolayer.

Figure 2A and B presents the compression–decompression

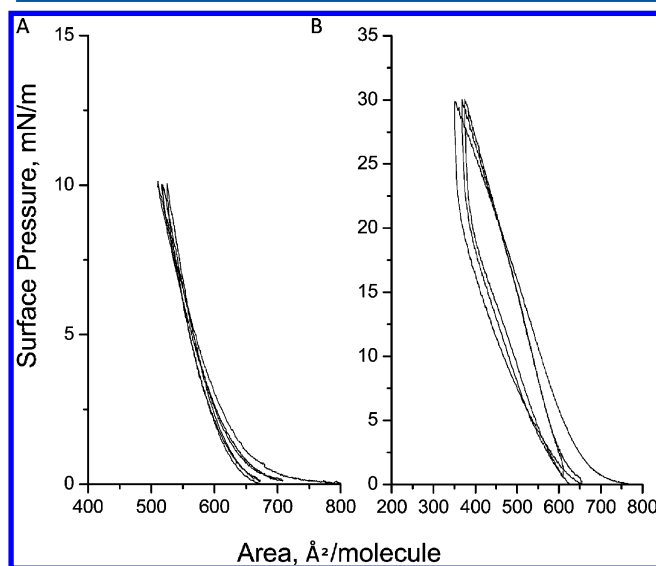


Figure 2. Three compression–decompression cycles up to a surface pressure of 10 (A) and 30 mN m^{-1} (B) of human insulin Langmuir monolayer at subphase pH 5.6.

cycle isotherms measured at two target surface pressures, namely, 10 and 30 mN m^{-1} . The rationale to choose these two surface pressures was to observe the stability of the film in a liquid condensed film before and after the collapse surface pressure. After the compression–decompression cycles from 0 up to 10 and 30 mN m^{-1} , one observes a variation of less than 5 and 10% between the initial compression and last decompression (third cycle), respectively. This result indicates that the HI protein remains at the interface. It has to be mentioned that the cycles up to 10 mN m^{-1} showed an overlap of the isotherms which supports the interpretation that the insulin protein might keep its conformation in the liquid expanded and condensed phases. Regarding the stability of the HI Langmuir monolayer (Figure 3), one has observed the decrease in area with time when the monolayer was kept constant at 10 and 30 mN m^{-1} during a 6500 s time period. A

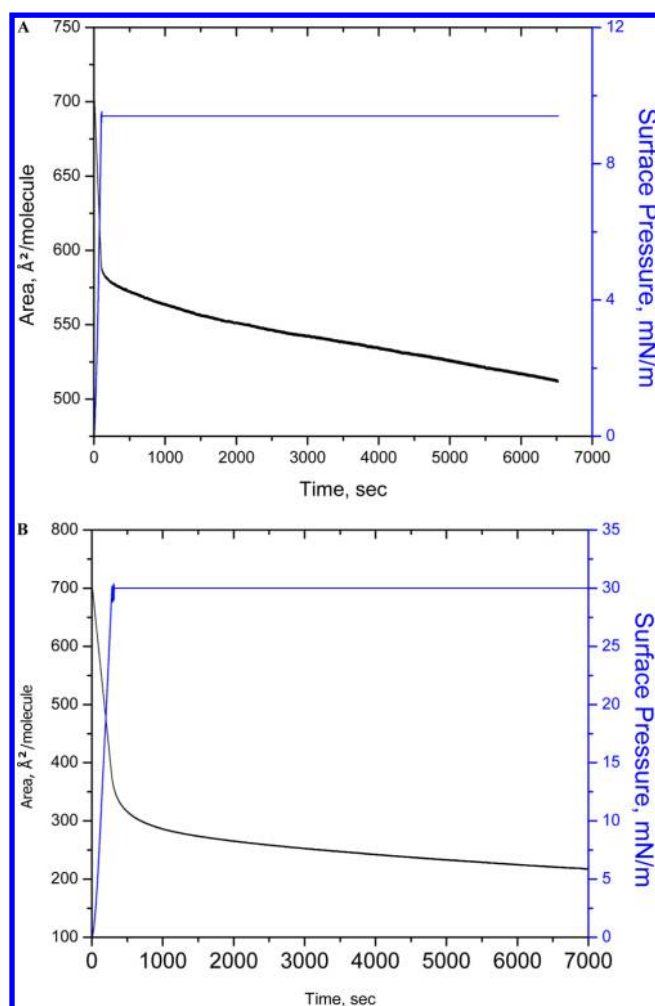


Figure 3. Stability measurements at surface pressures of 10 (A) and 30 mN/m (B) held for 90 min for human insulin Langmuir monolayer at subphase pH 5.6.

decrease of 15 and 60% was measured for the 10 and 30 mN m^{-1} , respectively. One would expect a large decrease at the collapse surface pressure after collapse. Possibility of aggregation of HI was studied by BAM, and conjugating HI with FITC, and will be discussed later.

3.3. UV-vis and Fluorescence Spectroscopy of Human Insulin in Aqueous Phase and Langmuir Monolayer. The photophysical properties of the HI were investigated in aqueous solution (pH 2) and as a Langmuir monolayer, as shown in Figures 4 and 5, respectively. Figure 4 includes both the absorbance and emission spectra of human insulin in solution. The emission peak of aqueous HI (pH 2) was observed at 305 nm when excited at 270 nm. This peak corresponds to the four tyrosine amino acids present in HI. This value is comparable with values obtained in other work at pH 7, i.e., 303–305 nm.²¹ However, at the air–water interface, no fluorescence was observed when excited at 270 nm (Figure 5B). The only peak observed was the Raman peak at 294 nm. This can be explained by the low concentration of HI (0.3 mg/mL) which is required for generating a surface pressure isotherm. Therefore, no correlation or comparison can be made between the fluorescence spectrum of HI as a Langmuir monolayer and in solution due to absence of fluorescence of HI as a Langmuir monolayer.

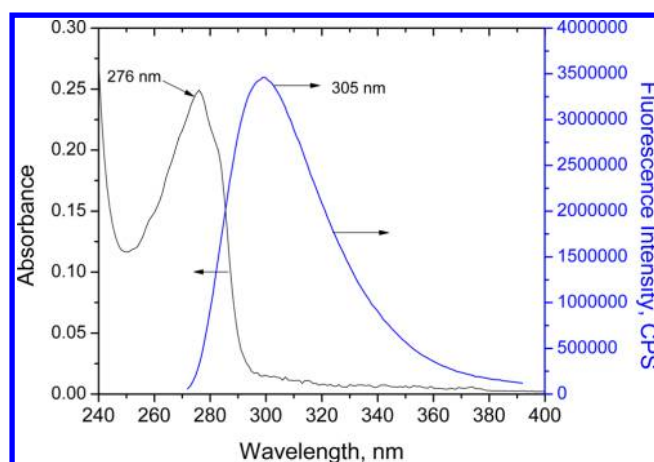


Figure 4. UV-vis (5×10^{-5} M) and fluorescence (5×10^{-7} M; $\lambda_{\text{excitation}} = 270$ nm, slit width at the excitation and emission, 5 and 5 nm, respectively) spectra of aqueous solution of human insulin.

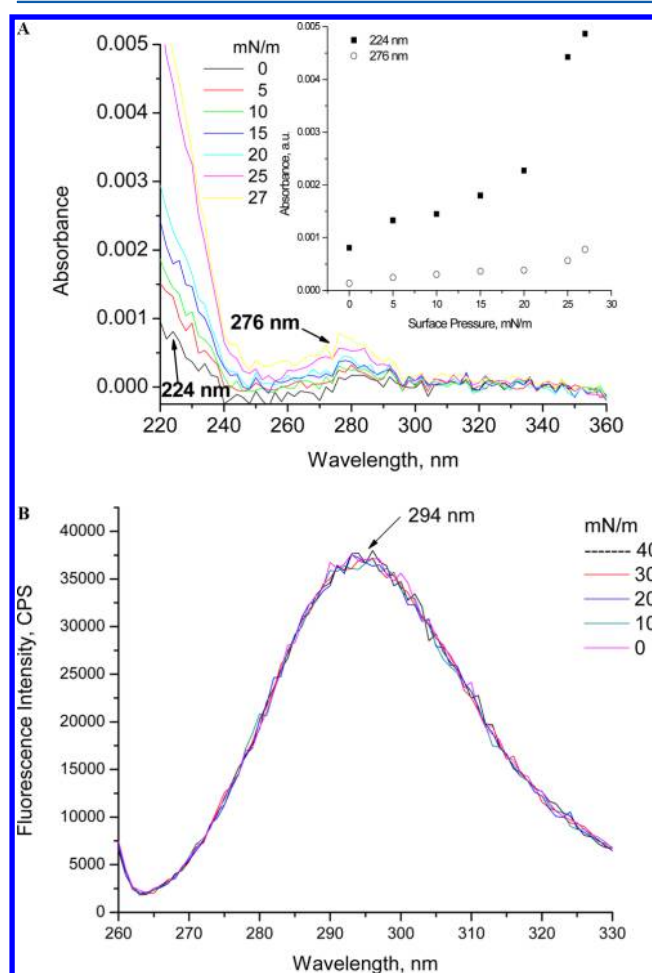
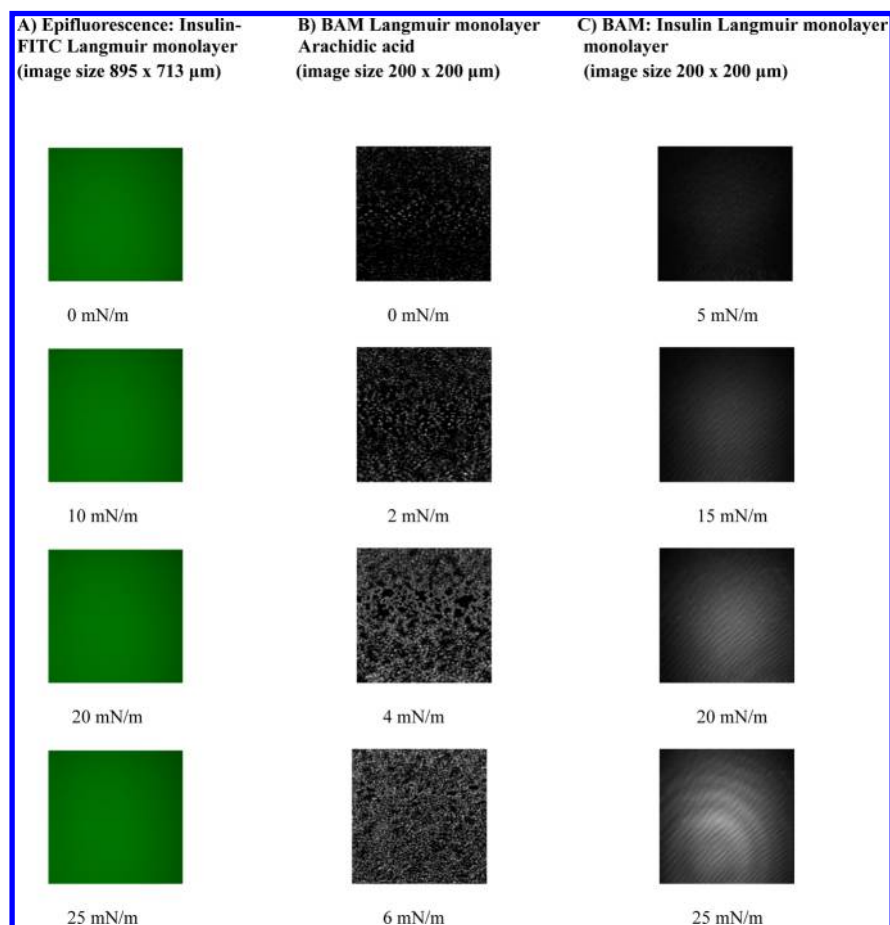


Figure 5. (A) UV-vis spectra of human insulin Langmuir at subphase pH 5.6. The inset shows the variation of the absorbance at 224 and 276 nm as a function of the surface pressure. (B) Fluorescence spectra of human insulin Langmuir ($\lambda_{\text{excitation}} = 270$ nm, slit width at the excitation and emission, 5 and 5 nm, respectively) at subphase pH 5.6.

Usually proteins show a peak for the aromatic amino acid present in them around 260–280 nm and a peak near 220 nm which is due to peptide bond. The spectra shown in Figure 5A presents a peak at 276 nm in the UV-vis spectra which is due

Table 1. Four Surface Pressures Were Measured by (A) Epifluorescence for a Sample of HI-FITC Langmuir Monolayer; (B) BAM for Insulin HI Langmuir Monolayer; (C) BAM for Arachidic Acid Langmuir Monolayer (Insulin Concentration: 0.30 mg/mL)



to the presence of tyrosine in the protein. Besides the peak at 276 nm, proteins are expected to have an intense peak at 190 nm and a weak peak between 210 and 220 nm due to the peptide bond. In solution, the only peak observed for human insulin was at 276 nm. Different concentrations of human insulin in solution yielded a spectrum with a broad shoulder near 200–220 nm which indicates that the peaks due to the peptide bond are overlapping. Figure 5A presents the absorbance spectra of the human insulin Langmuir monolayer. At the air–water interface, two distinct peaks at 224 and 276 nm were observed which represent the peptide bond and the tyrosine present in human insulin. When these two peaks are plotted against increasing surface pressure, they have a linear relationship. Linearity in absorbance at the air–water interface indicates stability of the HI monolayer until the collapse point.

The next section will look at the topography of the HI Langmuir monolayer in regard to the potential formation of domains in 2-D. Two methodologies were used for this observation, namely, epifluorescence and Brewster angle microscopy.

3.4. Epifluorescence and Brewster Angle Microscopy of Human Insulin Langmuir Monolayer. The topography of the human insulin Langmuir monolayer was examined using epifluorescence of the FITC-human insulin, whereas Brewster angle microscopy was employed for pure human insulin in 2-D. Since insulin is nonfluorescent, one must attach a fluorophore to make use of the epifluorescence microscopy. The probe

commonly used for proteins is fluorescein isothiocyanate (FITC).

Knowing the ratio of FITC-insulin (1:1), the molecular weight was calculated to prepare the right concentration of aqueous solution to be spread at the air–water interface. Epifluorescence micrography was obtained at surface pressures of 5, 10, 20, and 30 mN m^{-1} , as shown in Table 1. A homogeneous HI Langmuir monolayer was observed at all surface pressures without any indication of the formation of domains in the μm range in the images. To verify this observation, Brewster angle microscopy (BAM) was employed to image the topography of the film at the same pressure as the epifluorescence ones. The BAM data confirms the epifluorescence measurements. To ensure that the BAM system worked properly, the arachidic acid-Langmuir monolayer was examined. The topography observed corroborates the results already published (Table 1).²³

3.5. Secondary Structure of Insulin. To examine the nature of the interaction between insulin molecules in 2-D, the HI aqueous phase and Langmuir monolayer were examined by infrared spectroscopy. The FTIR and circular dichroism (CD) was studied for the HI aqueous phase, whereas infrared reflection absorption spectroscopy (IRRAS) was used for the HI Langmuir monolayer.

As shown in Figure 6A, the CD spectrum contains a high proportion of α -helix compared with β -sheet. It indicates the presence of monomers and absence of aggregates in the

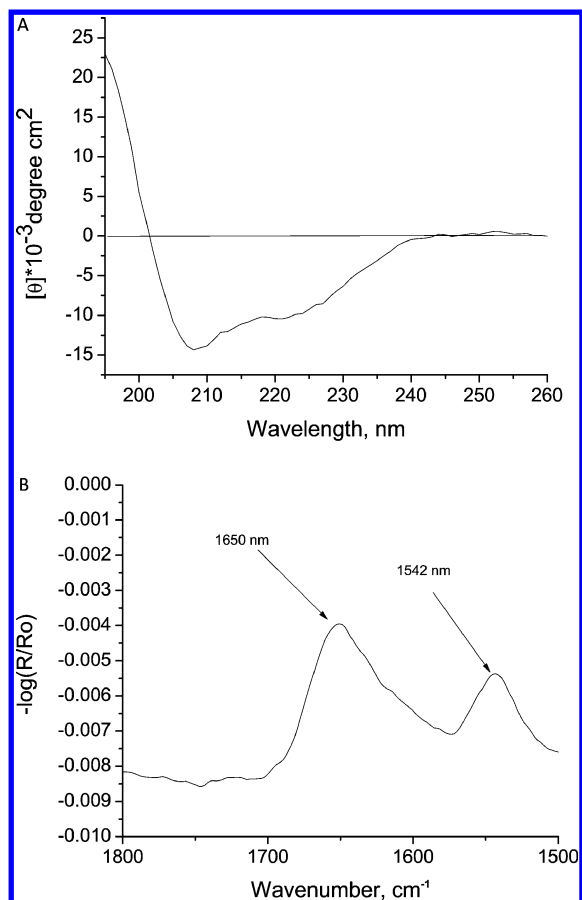


Figure 6. (A) Circular dichroism spectrum and (B) FTIR spectrum of aqueous insulin at pH 2 and temperature 20 ± 1 °C. The concentration of the insulin was 0.3 and 2 mg mL^{-1} , respectively.

aqueous phase.²⁴ Figure 6B shows the FTIR spectrum of aqueous HI with major peaks at 1650, 1542, 1440, and 1373 cm^{-1} . Peaks at 1650 and 1542 cm^{-1} correspond to amide I and amide II regions of α -helix.^{25–27} CD and FTIR spectra confirm that the aqueous HI exists as an α -helix, hence as a monomer in an aqueous phase.

IRRAS is an important technique to study the orientation and conformation changes of Langmuir monolayer at the air–water interface. IRRAS measurements were obtained as reflectance–absorbance (RA) vs wavenumber. RA is defined as $-\log_{10}(R/R_F)$, where R is the reflectivity of the film covered surface and R_F is the reflectivity of the water.^{28–30} When the vibrations are parallel to the air–water interface, for p-polarized radiation, which is parallel to the plane of incidence, the bands are initially negative and their intensities increase as the incident angle is increased until the Brewster angle (54.5° for 2920 cm^{-1} of IR radiation) is reached.³⁰ By using IRRAS at different surface pressures, we investigated the change of orientation and conformation of the HI Langmuir monolayer (Figures 7, 8, and 9). IRRAS was used to analyze structural features of the proteins, such as α -helix and β -sheet interpreted through amide I and amide II bands in the regions 1700–1600 and 1600–1500 cm^{-1} , respectively.^{19,20}

Three IRRAS spectra are presented. Figure 7 shows p-polarization at 60° at various surface pressures, Figure 8 shows a constant surface pressure of 10 mN/m and varying angles in a range from 30 to 70° , and Figure 9 shows s-polarization at a constant angle of 25° with varying surface pressures. Table 2

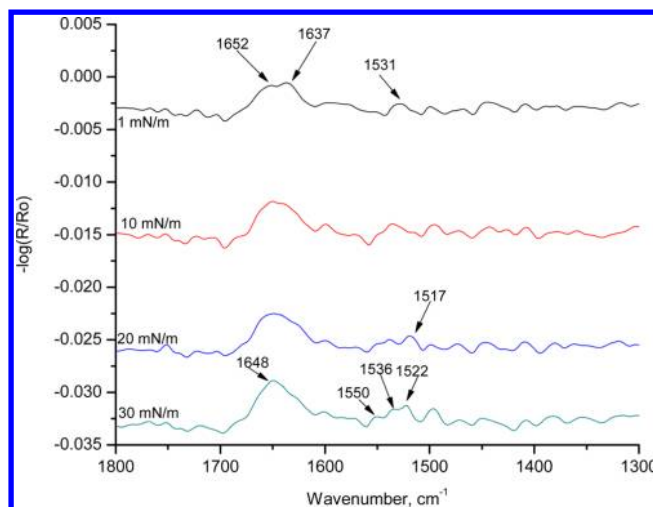


Figure 7. p-Polarized IRRAS of human insulin Langmuir monolayer at subphase pH 5.6 using an incident angle of 60° , and varying the surface pressures.

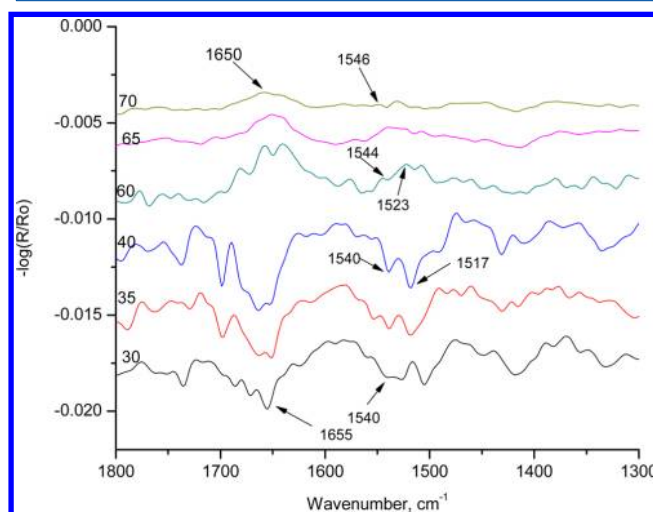


Figure 8. p-Polarized IRRAS of human insulin Langmuir monolayer at subphase pH 5.6 and surface pressure 10 mN/m , and varying the incident angles.

gives the bands characteristic of α -helix and β -sheet and amide I and amide II vibrations corresponding to α -helix.

Figure 7 shows p-polarization of the HI Langmuir monolayer at 60° at various surface pressures. The band at 1517 cm^{-1} corresponds to α -helix. At a surface pressure of 1 mN/m , there are two visible bands: 1652 and 1637 cm^{-1} . With increasing surface pressure, the two bands overlap and become a broad band. At 30 mN m^{-1} , the band is visible as a single band with frequency at 1648 cm^{-1} . This is the band corresponding to the amide I region of the α -helix. The next band appears as a broad band at 1 mN/m at 1531 cm^{-1} . With increasing surface pressure, it breaks into three bands: 1550, 1536, and 1522 cm^{-1} . The bands at 1550 and 1522 cm^{-1} correspond to the amide II region in the α -helix and β -sheet, respectively. This splitting of bands suggests that the band present at 1531 cm^{-1} at lower surface pressures is composed of both α -helix and β -sheet. At higher surface pressure, the band separates into discrete individual peaks. The other peaks present in the spectra are due to the presence of amino acids and alkane chains. The band at 1448 cm^{-1} corresponds to C–H scissoring of CH_2 and

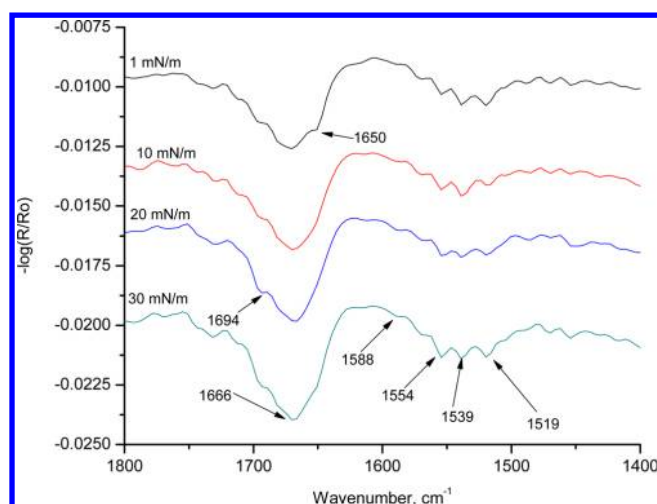


Figure 9. s-Polarized IRRAS of human insulin Langmuir monolayer at subphase pH 5.6 and an incident angle of 25°, and varying the surface pressures.

Table 2. Major Band Positions Characteristic of α Helix and β Sheet and IR Vibrations of Amide I and Amide II

protein structure	wavenumber (cm^{-1})
α helical structure	amide I absorption: 1650–1657 cm^{-1}
	amide II absorption: 1545–1551 cm^{-1}
β sheet structure	1515 cm^{-1}
	1628–1635 cm^{-1}
	1524–1525 cm^{-1}
	1690 cm^{-1}

CH_3 . All three major bands indicative of α -helix are present in the p-polarization IRRAS of the HI Langmuir monolayer.

Figure 8 shows p-polarization of the HI Langmuir monolayer at 10 mN m^{-1} at six different angles of 30, 35, 40, 60, 65, and 70°. Before Brewster angle, the angles at 30, 35, and 40 mN/m show none of the bands characteristic of β -sheet. All three angles show bands at 1655 and 1540 cm^{-1} which correspond to amide I and amide II absorption, respectively. The band at 1517 cm^{-1} , which corresponds to α -helix is present in 35 and 40°. After the Brewster angle, all three angles of 60, 65, and 70° show a band between 1650 and 1655, which corresponds to amide I absorption in α -helix. At an angle of 60°, a peak is visible at 1523 cm^{-1} , which corresponds to β sheet. None of the other bands present in the spectra are characteristic of α -helix or β -sheet. The spectra suggest that HI is in the form of α -helix at the air–water interface. With increasing angle at a constant pressure of 10 mN m^{-1} , the α -helix character is found to decrease in the spectra.

The s-polarization IRRAS of the HI Langmuir monolayer obtained at different surface pressures is presented in Figure 9. At a surface pressure of 1 mN m^{-1} , a band is present at 1650 cm^{-1} which corresponds to α -helix. With increasing surface pressure, this band disappears and merges into the band at 1666 cm^{-1} . The band at 1666 cm^{-1} includes β -turn and α -helix. The band at 1694 cm^{-1} corresponds to β -sheet. The band at 1519 cm^{-1} also corresponds to α -helix. The band observed at 1670 at an incident angle of 60° may be assigned to the sterically constrained C=O moiety present in β -turn or split in the peak is noticed due to transition dipole coupling in β -sheet. While varying the surface pressure, the most intense bands appeared at 1554 and 1539 cm^{-1} , both bands corresponding to

α -helix in amide II region. All three major bands are indicative of α -helix in the s-polarization IRRAS of the HI Langmuir monolayer.

From the above CD, FTIR, and IRRAS data, it can be concluded that HI dissolved in pH 2 exists in a helical conformation in solution and at the air–water interface.

4. CONCLUSION

The surface chemistry of a HI Langmuir monolayer was studied by surface pressure– and surface potential–area isotherms, and in situ spectroscopic measurements, namely, by UV–vis and fluorescence. The presence of the amino acid tyrosine resulted in insulin's characteristic absorbance and fluorescence spectra. The surface chemistry of the HI Langmuir monolayer indicates a stable HI monolayer until collapse at 25.2 mN m^{-1} , as shown by UV–vis and stability studies at the air–water interface. Microdomain formation of HI monolayer was examined by epifluorescence of HI-FITC and BAM. In both cases, a homogeneous HI Langmuir monolayer was observed at all surface pressures without any indication of the formation of domains in the μm range in the topography of the film. The secondary structure of the HI in solution and at the air–water interface was examined by IRRAS. The data were interjected for both phases as a high α -helix content, which mainly indicates the presence of monomers in the HI Langmuir monolayer.

AUTHOR INFORMATION

Corresponding Author

*Phone: +1 305 284 2194. Fax: +1 305 284 4571. E-mail: rml@miami.edu.

Notes

The authors declare no competing financial interest.

ACKNOWLEDGMENTS

This study was supported by NSF Eager Award CBET-0944290. We would like to thank Lisa Joseph for assistance in the preparation of HI-FITC conjugate.

REFERENCES

- (1) Bliss, M. *The Discovery of Insulin*; University of Chicago Press: Chicago, IL, 1982.
- (2) Baker, E.; Blundell, L.; Cutfield, J.; Cutfield, S.; Dodson, E.; Dodson, G.; Hodgkin, D.; Hubbard, R.; Isaacs, N.; Reynolds, C.; Sakabe, K.; Sakabe, N.; Vijayan, N. *Philos. Trans. R. Soc. London, Ser. B* **1988**, 319 (1195), 369–4956.
- (3) Nieto-Suarez, M.; Villa-Romeu, N.; Prieto, I. *Thin Solid Films* **2007**, 516, 8873–8879.
- (4) Bowen, R.; Austgen, L.; Rouge, M. *The structure of insulin*. http://www.vivo.colostate.edu/hbooks/pathophys/endocrine/pancreas/insulin_struct.html (Jan 20, 2011).
- (5) Jiménez, J.; Nettleton, E.; Bouchard, M.; Robinson, C.; Dobson, C.; Saibil, H. *Proc. Natl. Acad. Sci. U.S.A.* **2002**, 99 (14), 9196–9201.
- (6) Sunde, M.; Serpell, L.; Bartlam, M.; Fraser, P.; Pepys, M.; Blake, C. *J. Mol. Biol.* **1997**, 273 (3), 729–739.
- (7) Gaines, G. L., Jr. *Insoluble Monolayers at the Liquid–Gas Interfaces*; Interscience: New York, 1966.
- (8) Maget-Dana, R. *Biochim. Biophys. Acta, Rev. Biomembr.* **1999**, 1462 (1–2), 109–140.
- (9) Nagle, J. F. *J. Membr. Biol.* **1976**, 27 (1), 233–250.
- (10) Ganim, Z. *Phys. Chem. Chem. Phys.* **2010**, 12 (14), 3579–3588.
- (11) Harrap, B. S. *J. Coll. Sci., Imp. Univ. Tokyo* **1954**, 9 (6), 522–534.
- (12) Llopis, J.; Rebollo, D. V. *Arch. Biochem. Biophys.* **1959**, 88 (1), 142–149.

- (13) Kaka, M. S.; Pak, C. Y. C. *J. Gen. Physiol.* **1969**, *54* (1P1), 134–143.
- (14) Birdi, K. S. *J. Colloid Interface Sci.* **1976**, *57* (2), 228–232.
- (15) Schwinke, L. D.; Ganesan, M. G.; Weiner, N. D. *J. Pharm. Sci.* **2006**, *72* (3), 244–248.
- (16) Kozarac, Z.; Dhathathreyan, A.; Mobius, D. *Colloids Surf.* **1988**, *33*, 11–24.
- (17) Nieto-Suarez, A.; Vila-Romeu, N.; Dynarowicz-Latka, P. *Colloids Surf., A* **2008**, *321* (1–3), 189–198.
- (18) Balashev, K.; Ivanova, T.; Mircheva, K.; Panaiotov, I. *J. Colloid Interface Sci.* **2011**, *360*, 654–661.
- (19) Dluhy, R. A. *Spectrosc. Rev.* **2000**, *35* (4), 315–351.
- (20) Mendelson, R.; Brauner, J.; Gericke, A. *Annu. Rev. Phys. Chem.* **1998**, *46*, 305–334.
- (21) Santos, N. C.; Castanho, M. *Trends Appl. Spectrosc.* **2002**, *4*, 113–125.
- (22) Jobbagy, A.; Kiraly, K. *Biochim. Biophys. Acta* **1966**, *124*, 166–175.
- (23) Fainerman, V. B.; Vollhardt, D.; Johann, R. *Langmuir* **2000**, *16* (20), 7731–7736.
- (24) Provencher, S. W.; Gloeckner, J. *Biochemistry* **1981**, *20*, 33–37.
- (25) Bouchard, M.; Zurdo, J.; Nettleton, E.; Dobson, C.; Robinson, C. *Protein Sci.* **2000**, *9*, 1960–1967.
- (26) Wei, J.; Lin, Y.; Zhou, J.; Tsou, C. *Biochim. Biophys. Acta, Protein Struct.* **1991**, *1080* (1), 29–33.
- (27) Jackson, M.; Mantsch, H. *Crit. Rev. Biochem. Mol. Biol.* **1995**, *30* (2), 95–120.
- (28) Du, X.; Miao, W.; Liang, Y. *J. Phys. Chem. B* **2005**, *109* (15), 7428–7434.
- (29) Thakur, G.; Leblanc, R. M. *Langmuir* **2009**, *25* (5), 2842–2849.
- (30) Dluhy, R. A.; Cornell, D. G. *J. Phys. Chem.* **1985**, *89*, 3195–3197.